Josephson radiation and shot noise of a semiconductor nanowire junction

David J. van Woerkom,[1,2] Alex Proutski,[1,2] Ruben J. J. van Gulik,[1,2] Tamás Kriváchy,[1,2] Diana Car,[3] Sébastian R. Plissard,[3,2] Erik P. A. M. Bakkers,[1,2,3] Leo P. Kouwenhoven,[1,2] and Attila Geresdi[1,2,*]

[1] *QuTech, Delft University of Technology, 2600 GA Delft, The Netherlands*
[2] *Kavli Institute of Nanoscience, Delft University of Technology, 2600 GA Delft, The Netherlands*
[3] *Department of Applied Physics, Eindhoven University of Technology, 5600 MB Eindhoven, The Netherlands*

(Dated: February 10, 2017)

We measured the Josephson radiation emitted by an InSb semiconductor nanowire junction utilizing photon assisted quasiparticle tunneling in an AC-coupled superconducting tunnel junction. We quantify the action of the local microwave environment by evaluating the frequency dependence of the inelastic Cooper-pair tunneling of the nanowire junction and find the zero frequency impedance $Z(0) = 492\,\Omega$ with a cutoff frequency of $f_0 = 33.1\,\mathrm{GHz}$. We extract a circuit coupling efficiency of $\eta \approx 0.1$ and a detector quantum efficiency approaching unity in the high frequency limit. In addition to the Josephson radiation, we identify a shot noise contribution with a Fano factor of $F = 0.88$ which is consistent with the presence of single electron states in the nanowire channel.

The tunneling of Cooper pairs through a junction between two superconducting condensates gives rise to a dissipationless current [1] with a maximum amplitude of the critical current, I_c [2]. Upon applying a finite voltage bias V, the junction becomes an oscillating current source

$$I_s(t) = I_c \sin(2\pi f t), \tag{1}$$

with a frequency set by $hf = 2eV$ where h is the Planck constant and e is the electron charge.

The Josephson radiation, defined by Eq. (1) has mostly been investigated for superconducting tunnel junctions [3–5], metallic Cooper-pair transistors [6] and in circuit QED geometries [7]. Recently, it has also been proposed as a probe for topological superconductivity [8–10], which requires gateable semiconductor Josephson junctions [11].

In contrast to superconductor-insulator-superconductor (SIS) junctions, Josephson junctions with a semiconductor channel feature conductive modes of finite transmission probabilities [12, 13], leading to deviations from a sinusoidal current-phase relationship [14] and the universal ratio of the critical current and the normal state conductance [2]. Furthermore, soft-gap effects [15] have been shown to result in excess quasiparticle current for subgap bias voltages, limiting prospective applications such as topological circuits [16] and gate-controlled transmon qubits [17].

Here we investigate the high frequency radiation signatures of a voltage-biased semiconductor Josephson junction [11] by directly measuring the frequency-resolved spectral density for the first time. As a frequency-sensitive detector, we utilize a SIS junction, where the photon-assisted tunneling current [5] is determined by the spectral density of the coupled microwave radiation [18]. In addition to the detection of the monochromatic Josephson radiation, we demonstrate the presence of a broadband contribution, attributed to the shot noise of the nanowire junction [19].

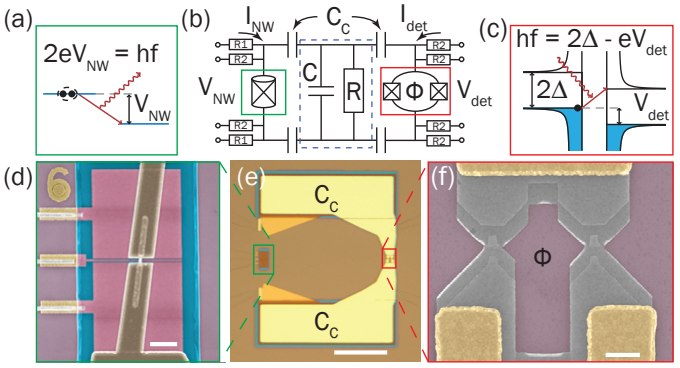

FIG. 1. (Color online) (a) Photon emission due to the inelastic Cooper-pair tunneling between condensate levels shifted by the bias voltage, V_{NW}. (b) The microwave equivalent circuit of the measurement setup, where R and C in the blue dashed box represent the microwave losses and stray capacitance, yielding a $2\pi f_0 = (RC)^{-1}$ upper cutoff frequency. The $C_c \gg C$ coupling capacitors have a negligible effect above a frequency of $2\pi f_c = (RC_c)^{-1}$ with $f_c \ll f_0$, but allow for the application of independent DC bias voltages V_{NW} and V_{det}. The $I_{\mathrm{NW}}(V_{\mathrm{NW}})$ and $I_{\mathrm{det}}(V_{\mathrm{det}})$ characteristics are measured through the Pt feedline resistors, depicted by R_1 and R_2. (c) Photon-assisted quasiparticle tunneling for a detector voltage bias V_{det} and an incoming photon energy of hf. (d) False colored scanning electron micrograph of the nanowire Josephson junction contacted with NbTiN after being placed on three electrostatic gates. (e) Bright field optical image of the coupling circuitry before the NbTiN deposition step with the nanowire junction (green box) and the detector junction (red box). (f) False colored micrograph of the detector split junction with an applied magnetic flux Φ. The scale bars depict $1\,\mu\mathrm{m}$ (d), $20\,\mu\mathrm{m}$ (e) and $0.5\,\mu\mathrm{m}$ (f), respectively.

Our setup follows the geometry of earlier experiments utilizing SIS junctions [5]. In contrast, our microwave ra-

* Corresponding author; e-mail: a.geresdi@tudelft.nl

diation source is an InSb nanowire [20] Josephson junction (Fig. 1d) with a channel length of 100 nm. The junction leads (in brown in Fig. 1d) are created by removing the surface oxides by Ar ion milling and then *in-situ* sputtering of NbTiN superconducting alloy. Owing to the highly transparent contacts, this procedure enables induced superconductivity in the semiconductor channel [16, 17]. A predefined gate structure (purple regions in Fig. 1d) provides electrostatic control of the semiconductor channel and is covered by sputtering a 20 nm thick SiN_x dielectric layer.

The $I(V)$ characteristics of the two junctions are measured in a standard four point probe geometry via highly resistive Pt feedlines effectively decoupling the on-chip elements (Fig. 1) thermally anchored at 20 mK from the measurement setup. In order to gain access to a wider $V_{\rm NW}$ range, we use $R_1 = 1\,\mathrm{k\Omega}$ in the nanowire biasing lines and $R_2 = 12\,\mathrm{k\Omega}$ in the voltage measurement leads (see Fig. 1b).

The detector SIS split junction is shown in Fig. 1f and is fabricated using standard shadow evaporation techniques [21]. The typical normal state resistance was measured to be $20\,\mathrm{k\Omega}$ for a nominal junction area of $100 \times 100\,\mathrm{nm}^2$. The bottom and top Al layer thicknesses are 9 and 11 nm, respectively. The split junction geometry enables the flux control of the total Josephson coupling of the detector. To measure the quasiparticle tunneling response, we set $\Phi = \Phi_0/2$, with $\Phi_0 = h/2e$ the flux quantum, to minimize the Josephson coupling. Finally, we utilize two parallel plate capacitors of $C_c \approx 400\,\mathrm{fF}$ with sputtered SiN_x dielectric which couple the nanowire junction to the detector in the frequencies of interest (Fig. 1e), yet enable independent voltage biasing and current measurements in the DC domain.

The mesoscopic noise source under consideration is characterized by its current noise density, $S_I(f)$ [19], which results in the voltage noise density $S_V(f) = S_I(f)|Z(f)|^2$, where $Z(f)$ is the complex frequency-dependent impedance of the coupling circuit. In Fig. 1b, we depict a parallel RC network resulting in $Z(f) = R(1-jf/f_0)/(1+f^2/f_0^2)$ with $2\pi f_0 = (RC)^{-1}$ in the limit of negligible detector admittance, $r_{\rm det}^{-1} = dI_{\rm det}/dV_{\rm det} \ll R^{-1}$.

We deduce the voltage noise density $S_V(f)$ starting from the equation for the photon-assisted current in the SIS detector [5, 22]:

$$I_{\rm PAT}(V_{\rm det}) = \int_0^\infty S_V(f) \left(\frac{e}{hf}\right)^2 I_{QP,0}\left(V_{\rm det} + \frac{hf}{e}\right) \mathrm{d}f, \tag{2}$$

which describes the DC current contribution at an applied voltage $V_{\rm det} < 2\Delta$. Crucially, this equation holds if the quasiparticle current in the absence of radiation has a well-defined onset, $I_{QP,0}(V_{\rm det} < 2\Delta) = 0$, typically referred to as the quantum limit of the detector [22] and in the limit of weak coupling, where multiphoton processes do not contribute [18]. Note that Eq. (2) can be handled as a convolution of $S_V(f)/(hf)^2$ and $I_{QP,0}(V_{\rm det})$.

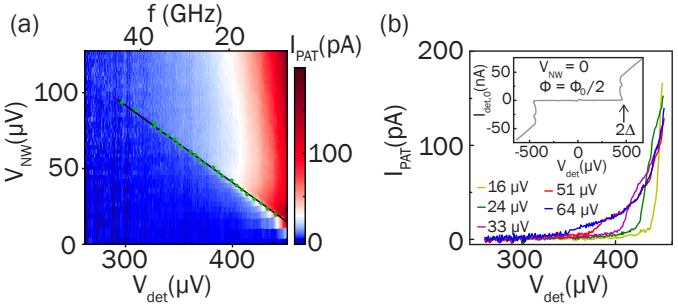

FIG. 2. (Color online) (a) Measured photon-assisted quasiparticle current $I_{\rm PAT}$ as a function of the detector bias voltage $V_{\rm det}$ and nanowire bias voltage $V_{\rm NW}$. The green dots denote the extracted frequency on the upper axis for a given $V_{\rm NW}$. The solid black line is the best linear fit with $f/V_{\rm NW} = 475\,\mathrm{MHz}/\mu\mathrm{V}$. (b) Horizontal line traces at different $V_{\rm NW}$ values. The inset shows the full $I_{\rm det,0}(V_{\rm det})$ characteristics of the detector when the Josephson radiation is absent. Note that the applied flux $\Phi = \Phi_0/2$ through the split junction results in a suppressed supercurrent branch. The arrow depicts $2\Delta/e = 480\,\mu\mathrm{V}$, the onset of the quasiparticle current.

In the presence of a monochromatic radiation, where $S_V(f) \sim \delta(f - \mathcal{F})$, Eq. (2) describes the shift of the initial $I_{QP,0}(V_{\rm det})$ quasiparticle current by $\delta V_{\rm det} = h\mathcal{F}/e$. This is the case of the Josephson radiation [5] with $S_I(f) = \frac{I_c^2}{4}\delta(f - \mathcal{F})$, where $h\mathcal{F} = 2eV_{\rm NW}$ with $V_{\rm NW}$ the applied voltage bias on the emitter junction with a critical current I_c. On the other hand, quasiparticle shot noise is characterized by a frequency-independent contribution of $S_I = 2eIF$ with I being the applied current and F the Fano factor which is characteristic to the mesoscopic details of the junction [19].

The impedance $Z(f)$ of the environment results in a finite power dissipation $I_c^2\mathrm{Re}(Z(f))/2$ which gives rise to a DC current due to inelastic Cooper-pair tunneling (ICPT) processes in the NW Josephson junction (see Fig. 1a) [4]. This effect has been first addressed to calculate the shape of the supercurrent branch in overdamped SIS junctions and purely resistive environments [23]. Later, the theory was adapted for high channel transmissions [24]. It also has been shown that for an arbitrary $Z(f) \ll h/4e^2 \approx 6.5\,\mathrm{k\Omega}$, the ICPT contribution can be evaluated as [4]

$$I_{\rm ICPT} = \frac{I_c^2\mathrm{Re}(Z(f))}{2V_{\rm NW}}, \tag{3}$$

with the critical current I_c and an applied voltage $V_{\rm NW}$. Here, the junction effectively probes the impedance $Z(f)$ at a frequency $f = 2eV_{\rm NW}/h$.

Importantly, the two independently measured current values $I_{\rm PAT}(V_{\rm det})$ and $I_{\rm ICPT}(V_{\rm NW})$ depend on the same

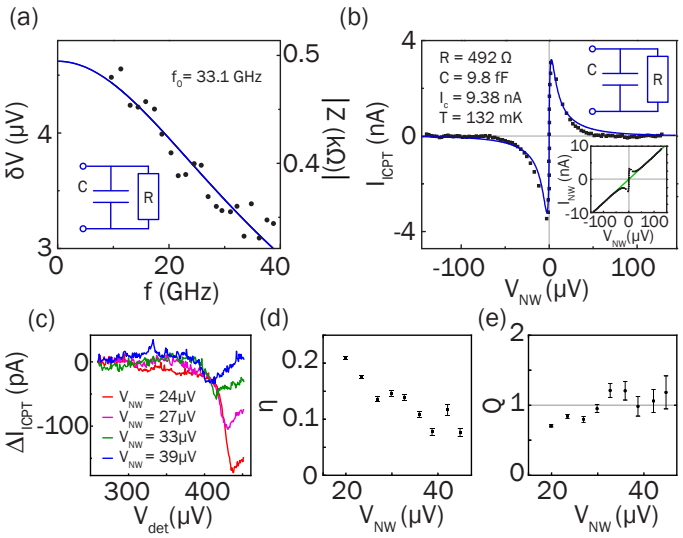

FIG. 3. (Color online) (a) The measured $\delta V(f) = I_c|Z(f)|$ voltage fluctuation on the detector junction. The solid line depicts the fitted cutoff with $2\pi f_0 = (RC)^{-1} = 33.1\,\mathrm{GHz}$. Right vertical axis shows the impedance $|Z(f)|$, see text. (b) Experimental $I_{\mathrm{ICPT}}(V_{\mathrm{NW}})$ trace of the nanowire junction exhibiting a current peak due to the supercurrent branch. The linear contribution with a resistance $R_{\mathrm{NW}} = 14.03\,\mathrm{k\Omega}$ (green solid line, see inset for raw $I_{\mathrm{NW}}(V_{\mathrm{NW}})$ trace) is subtracted. The blue solid line depicts the fitted curve with $I_c = 9.38\,\mathrm{nA}$ critical current and a noise temperature $T = 132\,\mathrm{mK}$. (c) Variation of the nanowire junction current ΔI_{ICPT} as a function of the detector voltage V_{det}. The extracted circuit efficiency η (d) and the detector quantum efficiency Q (e) as a function of V_{NW}, see text.

microwave environment, characterized by $Z(f)$. Thus, by evaluating both, we find $Z(f)$ and the Josephson coupling of the nanowire junction at the same time.

We demonstrate the detection of the Josephson radiation in Fig. 2. In panel (a) we plot the PAT current contribution as a function of the DC bias voltages V_{det} and V_{NW}. In Fig. 2b, we show line traces $I_{\mathrm{PAT}}(V_{\mathrm{det}})$ exhibiting well-defined onset values corresponding to a monochromatic Josephson radiation tuned by V_{NW}. Thus, we can deconvolute Eq. (2) to find the radiation frequency shown as green dots in Fig. 2a. We note however, that the measured $I_{\mathrm{det},0}$ plotted in the inset of Fig. 2b is distorted due to self-heating effects in the SIS detector. Thus, we used a monotonous $I_{QP,0}(V_{\mathrm{det}})$ centered around the same quasiparticle onset. For the details of the deconvolution algorithm, and raw data files, see [25].

By evaluating the relation between V_{NW} and the radiation frequency (black line in Fig. 2a), we find a ratio of $475\pm4.2\ \frac{MHz}{\mu V}$ which is in reasonable agreement with $\frac{2e}{h} \sim 484\frac{MHz}{\mu V}$ expected for the case of Cooper-pair tunneling [26]. The intersect for $f = 0$ is set by the quasiparticle current onset to be $2\Delta/e = 480\,\mu\mathrm{V}$ (see inset of Fig. 2b).

It is important to notice that the PAT current decreases with increasing frequency (Fig. 2b). By correcting for the $\sim f^{-2}$ dependence in Eq. (2), we find that the fluctuation amplitude $\delta V = I_c|Z(f)| \sim \sqrt{S_V}$ exhibits a characteristic cutoff frequency (Fig. 3a), even though the current oscillation amplitude of the Josephson junction is constant, see Eq. (1). Thus, we can attribute this cutoff to the coupling circuit impedance, $Z(f)$. We find a good agreement between the experimental data and the impedance of a single-pole RC network (solid blue line in Fig. 3a) yielding to a cutoff frequency $f_0 = (2\pi RC)^{-1} = 33.1\,\mathrm{GHz}$.

Next, we turn to the measured $I(V)$ trace of the nanowire Josephson junction. The inset of Fig. 3b shows the raw curve, which exhibits a supercurrent peak around zero V_{NW} and a linear branch. The latter fits to a linear slope of $R_{\mathrm{NW}} = 14.03\,\mathrm{k\Omega}$ (solid green line). We then extract the $I_{\mathrm{ICPT}}(V_{\mathrm{NW}})$ component by removing this slope (black dots in Fig. 3b). In order to find the critical current and the noise temperature of the junction, we use the finite temperature solution of Ivanchenko and Zil'bermann [23] with substituting $|Z(f)|$ as the impedance of the environment [25]. With this addition, we find an excellent agreement with the experimental data (blue solid line in Fig. 3b), with $I_c = 9.38\,\mathrm{nA}$ critical current. Notably, with the now determined value of I_c, we can extract $R = 492\,\Omega$ and $C = 9.8\,\mathrm{fF}$ fully characterizing the microwave environment of the junctions. In addition, we find $I_c R_{\mathrm{NW}} = 132\,\mu\mathrm{V}$, which is close to the induced gap values measured in similar devices [16]. We also extract an effective noise temperature $T = 132\,\mathrm{mK}$, which is higher than the substrate temperature of 20 mK, similarly to earlier experiments [24].

Thus far, we evaluated $I_{\mathrm{ICPT}}(V_{\mathrm{NW}})$ at $V_{\mathrm{det}} \approx 50\,\mu\mathrm{V} \ll 2\Delta/e = 480\,\mu\mathrm{V}$, where $I_{\mathrm{PAT}} \approx 0$, thus the detector load is negligible. However, depending on V_{NW}, we find a negative $\Delta I_{\mathrm{ICPT}}(V_{\mathrm{det}})$, i.e. a reduction of the emitter current, when the detector threshold is on resonance with the emitted frequency (Fig. 3c). We can understand this effect by the reduction of $Z(f)$ in Eq. (3) in the presence of a finite r_{det} in parallel with R. In first order, we find $\Delta I_{\mathrm{ICPT}}/I_{\mathrm{ICPT}} = -\mathrm{Re}(Z(f))/r_{\mathrm{det}} \approx -R/r_{\mathrm{det}}$. By using the measured DC current values, we evaluate the efficiency of the coupling circuit to be the ratio of the absorbed and emitted power $\eta = P_{\mathrm{det}}/P_{\mathrm{emi}} = 2I_{\mathrm{PAT}}/I_{\mathrm{ICPT}}$ (Fig. 3d). We find typical values spanning $0.1 - 0.2$, an order of magnitude improvement over earlier reported values [5, 27]. The decrease of η with increasing f is consistent with the low-pass nature of the coupling circuit. We also calculate the detector quantum efficiency $Q = P_{\mathrm{det}}/\Delta P_{\mathrm{emi}} = 2I_{\mathrm{PAT}}/\Delta I_{\mathrm{ICPT}}$ (Fig. 3e) and find values scattering around unity. This value directly measures the ratio of electron and photon rate passing the detector junction, thus confirms that it is in the quantum limit

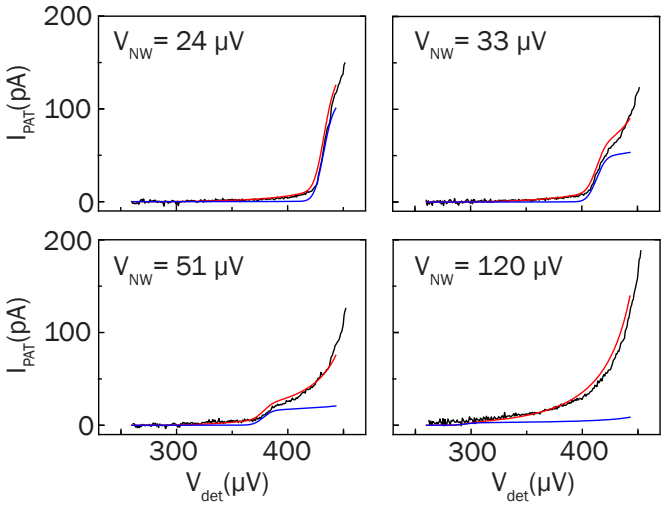

FIG. 4. (Color online) Detector $I_{\rm PAT}(V_{\rm det})$ line traces at various $V_{\rm NW}$ bias voltage values. The experimental data is shown by black lines. The blue lines depict the contribution of the Josephson radiation using the circuit parameters defined earlier. The red lines include the shot noise contribution with the sole global fit parameter $F = 0.88 \pm 0.11$, see text.

[22].

We now turn to the shot noise contribution to $I_{\rm PAT}$. We evaluate the measured data by including both $S_I \sim \delta(f - \mathcal{F})$ of the Josephson radiation, and $S_I = 2eIF$ of the shot noise with F being the Fano factor [19] in order to calculate $I_{\rm PAT}$ from Eq. (2). With setting $F = 0$, i.e. in the absence of shot noise, we find that the blue curves in Fig. 4 can fit the steps in $I_{\rm PAT}$, however fail to describe the smooth background of the dataset. A much better agreement is reached by using a single global fit parameter $F = 0.88 \pm 0.11$ (red curves in Fig. 4). We note that the channel length of 100 nm is similar to the mean free path found earlier in the same nanowires [28]. Thus the extracted Fano factor, yielding to sub-Poissonian shot noise, is consistent with the presence of several transport modes of low transmission τ, where $F = 1 - \tau$ assuming identical quasiballistic channels. In contrast, $F = 1/3$ characteristic of diffusive normal transport [29] does not fit our data.

Furthermore, the extracted Fano factor does not agree with the shot noise signature of multiple Andreev reflections, where $F > 1$ values are anticipated due to the transport of multiple charge quanta both in the ballistic [30] and in the diffusive [31] limit. Our experiment thus provides insight to the nature of the charge transport at finite voltage bias in the nanowire Josephson junction and concludes that the finite subgap current can be attributed to single electron states inside the induced superconducting gap.

In conclusion, we built and characterized an on-chip microwave coupling circuit to measure the microwave radiation spectrum of an InSb nanowire junction with NbTiN bulk superconducting leads. Our results clearly demonstrate the possibility of measuring the frequency of the Josephson radiation in a wide frequency range, opening new avenues in investigating the 4π-periodic Josephson effect [32] in the context of topological superconductivity [33]. Based on the Fano factor, the shot noise contribution to the measured signal demonstrates the presence of subgap quasiparticle states and excludes multiple Andreev reflection as the source of subgap current of the nanowire Josephson junction.

The authors acknowledge D. Bouman, A. Bruno, O. Benningshof, M. C. Cassidy, M. Quintero-Pèrez and R. Schouten for technical assistance and R. Deblock for fruitful discussions. This work has been supported by the Dutch Organization for Fundamental Research on Matter (FOM), the Netherlands Organization for Scientific Research (NWO) by a Veni grant, Microsoft Corporation Station Q and a Synergy Grant of the European Research Council.

[1] B. D. Josephson, Phys. Lett. **1**, 251 (1962).
[2] V. Ambegaokar and A. Baratoff, Phys. Rev. Lett. **10**, 486 (1963).
[3] I. Giaever, Phys. Rev. Lett. **14**, 904 (1965).
[4] T. Holst, D. Esteve, C. Urbina, and M. H. Devoret, Phys. Rev. Lett. **73**, 3455 (1994).
[5] R. Deblock, E. Onac, L. Gurevich, and L. P. Kouwenhoven, Science **301**, 203 (2003).
[6] P.-M. Billangeon, F. Pierre, H. Bouchiat, and R. Deblock, Phys. Rev. Lett. **98**, 126802 (2007).
[7] M. Hofheinz, F. Portier, Q. Baudouin, P. Joyez, D. Vion, P. Bertet, P. Roche, and D. Esteve, Phys. Rev. Lett. **106**, 217005 (2011).
[8] D. I. Pikulin and Y. V. Nazarov, Physical Review B **86**, 140504 (2012).
[9] P. San-Jose, E. Prada, and R. Aguado, Phys. Rev. Lett. **108**, 257001 (2012).
[10] M. Houzet, J. S. Meyer, D. M. Badiane, and L. I. Glazman, Phys. Rev. Lett. **111**, 046401 (2013).
[11] Y.-J. Doh, J. A. van Dam, A. L. Roest, E. P. A. M. Bakkers, L. P. Kouwenhoven, and S. De Franceschi, Science **309**, 272 (2005).
[12] J. Xiang, A. Vidan, M. Tinkham, R. M. Westervelt, and C. M. Lieber, Nature nanotechnology **1**, 208 (2006).
[13] D. J. van Woerkom, A. Proutski, B. van Heck, D. Bouman, J. I. Väyrynen, L. I. Glazman, P. Krogstrup, J. Nygård, L. P. Kouwenhoven, and A. Geresdi, arXiv preprint arXiv:1609.00333 (2016).
[14] M. L. Della Rocca, M. Chauvin, B. Huard, H. Pothier, D. Esteve, and C. Urbina, Phys. Rev. Lett. **99**, 127005 (2007).
[15] S. Takei, B. M. Fregoso, H.-Y. Hui, A. M. Lobos, and S. Das Sarma, Phys. Rev. Lett. **110**, 186803 (2013).
[16] V. Mourik, K. Zuo, S. M. Frolov, S. R. Plissard, E. P. A. M. Bakkers, and L. P. Kouwenhoven, Science **336**, 1003 (2012).
[17] G. de Lange, B. van Heck, A. Bruno, D. J. van Woerkom, A. Geresdi, S. R. Plissard, E. P. A. M. Bakkers, A. R.

Akhmerov, and L. DiCarlo, Phys. Rev. Lett. **115**, 127002 (2015).
[18] P. K. Tien and J. P. Gordon, Physical Review **129**, 647 (1963).
[19] Y. M. Blanter and M. Büttiker, Physics Reports **336**, 1 (2000).
[20] S. R. Plissard, D. R. Slapak, M. A. Verheijen, M. Hocevar, G. W. G. Immink, I. van Weperen, S. Nadj-Perge, S. M. Frolov, L. P. Kouwenhoven, and E. P. A. M. Bakkers, Nano Letters **12**, 1794 (2012).
[21] G. Dolan, Applied Physics Letters **31**, 337 (1977).
[22] J. R. Tucker and M. J. Feldman, Reviews of Modern Physics **57**, 1055 (1985).
[23] Y. M. Ivanchenko and L. A. Zil'berman, Sov. Phys. JETP **28**, 1272 (1969).
[24] M. Chauvin, P. vom Stein, D. Esteve, C. Urbina, J. C. Cuevas, and A. L. Yeyati, Phys. Rev. Lett. **99**, 067008 (2007).
[25] http://dx.doi.org/10.4121/uuid:b8c8d41b-1ede-4cf0-896e-1220411d63f4 Raw data and calculations.
[26] W. H. Parker, B. N. Taylor, and D. N. Langenberg, Phys. Rev. Lett. **18**, 287 (1967).
[27] P.-M. Billangeon, F. Pierre, H. Bouchiat, and R. Deblock, Phys. Rev. Lett. **96**, 136804 (2006).
[28] Ö. Gül, D. J. van Woerkom, I. van Weperen, D. Car, S. R. Plissard, E. P. Bakkers, and L. P. Kouwenhoven, Nanotechnology **26**, 215202 (2015).
[29] C. W. J. Beenakker and M. Büttiker, Phys. Rev. B **46**, 1889 (1992).
[30] R. Cron, M. F. Goffman, D. Esteve, and C. Urbina, Phys. Rev. Lett. **86**, 4104 (2001).
[31] T. Hoss, C. Strunk, T. Nussbaumer, R. Huber, U. Staufer, and C. Schönenberger, Phys. Rev. B **62**, 4079 (2000).
[32] R. M. Lutchyn, J. D. Sau, and S. Das Sarma, Phys. Rev. Lett. **105**, 077001 (2010).
[33] Y. Oreg, G. Refael, and F. von Oppen, Phys. Rev. Lett. **105**, 177002 (2010).